Int J Adv Manuf Technol (2001) 17:297–304

The International Journal of
Advanced
Manufacturing
Technology

Optimum Gate Design of FreeForm Injection Mould using the Abductive Network

J. C. Lin

Department of Mechanical Design Engineering, National Hu-Wei Institute of Technology, Yunlin, Taiwan

This study uses the injection position and size of the gate as the major control parameters for a simulated injection-mould. Once the injection parameters (gate size and gate position) are given, the product performance (deformation) can be accurately predicted by the abductive network developed.

To avoid the numerous influencing factors, first the part-line of the parameter equation is created by an abductive network to limit the range of the gate. The optimal injection parameters can be searched for by a simulation annealing (SA) optimisation algorithm, with a performance index, to obtain a perfect part. The major purpose is searching for the optimal gate location on the part-surface, and minimising the air-trap and deformation after part formation. This study also uses a practical example which has been and proved by experiment to achieve a satisfactory result.

Keywords: Abductive network; Injection mould; Simulation annealing (SA)

1. Introduction

Owing to the rapid development of industry and commerce in recent years, there is a need for rapid and high volume production of goods. The products are manufactured using moulds in order to save the time and cost. Plastic products are the majority. Owing to these products not requiring complicated processes it is possible to cope with market demand speedily and conveniently.

In traditional plastic production, the designs of the portions of the mould are determined by humans. However, because of the increased performance requirements, the complexity of plastic products has increased. First, the geometric shapes of the plastic products are difficult to draw, and the internal shape is often complex which also affects the production of the product.

Injection processing can be divided into three stages:

1. Heat the plastic material to a molten state. Then, by high pressure, force the material to the runner, and then into the mould cavity.
2. When the filling of the mould cavity is completed, more molten plastic should be delivered into the cavity at high pressure to compensate for the shrinkage of the plastic. This ensures complete filling of the mould cavity.
3. Take out the product after cooling.

Though the filling process is only a small proportion of the complete formation cycle, it is very important. If filling in incomplete, there is no pressure holding and cooling is required. Thus, the flow of the plastic fluid should be controlled thoroughly to ensure the quality of the product.

The isothermal filling model of a Newtonian fluid is the simplest injection mould-flow filling model. Richardson [1] produced a complete and detailed concept. The major concept is based on the application of lubrication theory, and he simplified the complex 3D flow theory to 2D Hele-Shaw flow. The Hele-Shaw flow was used to simulate the potential flow and was furthermore used in the plasticity flow of the plastic. He assumed the plasticity flow on an extremely thin plate and fully developed the flow by ignoring the speed change through the thickness. Kamal et al. used similar methods to obtain the filling condition for a rectangular mould cavity, and the analytical result obtained was almost identical to the experimental result.

Plastic material follows the Newtonian fluid model for flow in a mould cavity, and Bird et al. [2–4] derived mould-flow theory based on this. When the shape of a mould is complicated and there is variation in thickness, then the equilibrium equations changes to nonlinear and has no analytical solution. Thus, it can be solved only by finite-difference or numerical solutions [2,5]

Of course, as the polymer is a visco-elastic fluid, it is best to solve the flow problem by using visco-elasticity equations. In 1998, Goyal et al. used the White Metzner visco-elasticity model to simulate the disk mould-flow model for central pouring. Metzner, using a finite-difference method to solve the governing equation, fould the visco-elasticity effect would not change the distribution of speed and temperature. However, it affects the stress field very much. If it is a pure visco-elastic

Correspondence and offprint requests to: Dr. J. C. Lin, Department of Mechanical Design Engineering, National Hu-Wei Institute of Technology, Yunlin 632, Taiwan. E-mail: linrc@sunws.nhit.edu.tw

flow model, the popular GNF model is generally used to perform numerical simulation.

Currently, finite-element methods are mostly used for the solution of mould-flow problems. Other methods are pure visco-elastic models, such as C-FOLW and MOLD-FLOW software. We used this method as well. Some software employs the visco-elastic White–Metzner model, but it is limited to 2D mould-flow analysis. Simple mould flow analysis is limited by CPU time. For the complicated mould shapes, Papthanasion et al. used UCM fluid for filling analysis, using a finite-difference method and BFCC coordination system application for the solution of the more complicated mould-shape and filling problem, but it was not commercialised [6].

Many factors affect plastic material injection. The filling speed, injection pressure and molten temperature, holding pressure [7–12], cooling tube [13,14] and injection gate affect the accuracy of the plastic product, because, when the injection processing is completed, the flow of material in the mould cavity results in uneven temperature and pressure, and induces residual stress and deformation of the workpiece after cooling.

It is difficult to decide on the mould part-surface and gate positions. Generally, the mould part-surface is located at the widest plane of the mould. Searching for the optimal gate position depends on experience. Minimal modification to the mould is required if you are lucky. However, the time and cost required for the modification of most injection-moulds exceeds the original cost, if the choice of the part-line is poor. For the mould part surface, many workers used various methods to search for the optimal mould part-line, such as geometric shape and feature-based design [15–17]. Some workers used finite-element methods and abductive networks to look for the optimal gate design for a die-casting mould [18].

This study used an abductive network to establish the parameter relationship of the mould part-line, and used this formula for searching for 22 points on the injection mould part-line to serve as the location for an injection gate. Abductive networks are used to match injection pressure and pressure holding time to perform injection formation analysis, and to establish a relationship between these parameters, and the output result of the injection process.

It has been shown that prediction accuracy in abductive networks is much higher than that in other networks [19]. Abductive networks based on the abductive modelling technique are able to represent complex and uncertain relationships between mould-flow analysis results and injection parameters. It has beeen shown that the injection-strain and injection-stress in a product can be predicted, with reasonable accuracy, based on the developed networks. The abductive network has been constructed once the relationships of gate location that are input and simulated have been determined; an appropriate optimisation algorithm with a performance index is then used to search for the optimal location parameters.

In this paper, an optimisation method for simulated annealing [20] is presented. The simulated annealing algorithm is a simulation of the annealing process for minimising the performance index. It has been successfully applied to filtering in image processing [21], VLSI layout generation [22], discrete tolerance design [23], wire electrical discharge machining [24], deep-draw clearance [25], and casting-die runner design [26], etc. It provides an experimental foundation based on theory for the development and application of the technologies.

2. Mould-Flow Theory

The mould flow analysis include four major parts:

1. Filling stage.
2. Pressure holding stage.
3. Cooling and solidification stage.
4. Shrinkage and warp, i.e. stress residue stage.

Thus, the major mould flow equations are divided into four groups. In the filling stage, the mould cavity is filled with molten plastic fluid at high presssure. Thus, the governing equations include:

1. *Continuity equation*. The plastic deformation or shape change accompany the flow during the filling process (mass conservation):

$$\frac{\partial \rho}{\partial t} + \overline{\nabla} \bullet (\boldsymbol{\nabla} \mathbf{V}) = 0 \tag{1}$$

ρ = plastic density; V = vector velocity

2. *Momentum equation*. Newton's second law is used to derive the momentum (acceleration condition) or force balance generated by plastic flow:

$$\rho \left[\frac{\partial \mathbf{V}}{\partial t} + (\overline{V} \bullet \boldsymbol{\nabla}) \mathbf{V} \right] = - \mathbf{V} P + \boldsymbol{\nabla} \bullet \boldsymbol{\tau} + \rho f \tag{2}$$

P = flow pressure; f = body force; τ = stress tensor.

3. *Energy equation*. The energy conservation of system and laws of conservation of flow material, if the fluid is incompressible:

$$\rho C_P \left[\frac{\partial T}{\partial t} + (\mathbf{V} \bullet \boldsymbol{\nabla}) T \right] = - \boldsymbol{\nabla} \bullet q + \boldsymbol{\tau} : \boldsymbol{\nabla} \mathbf{V} \tag{3}$$

T = temperature; C_P = specific heat of constant pressure; q = heat flux

4. *Rheology equation*

$$\boldsymbol{\tau} = f_n(\dot{\boldsymbol{\gamma}}, T, P, \ldots) \tag{4}$$

$$\dot{\boldsymbol{\gamma}} = \boldsymbol{\nabla} \mathbf{V} + (\boldsymbol{\nabla} \mathbf{V})^T \tag{5}$$

∇V = deform tensor; $(\nabla V)^T$ = transport vector.

Holding pressure analysis. The holding pressure process is to maintain the pressure after the mould cavity is filled in order to inject more plastic, to compensate for the shrinkage in cooling.

$$\rho \frac{\partial V_1}{\partial t} = - \frac{\partial P}{\partial x_1} + \left[\frac{\partial \tau_{11}}{\partial x_1} + \frac{\partial \tau_{21}}{\partial x_2} + \frac{\partial \tau_{31}}{\partial x_3} \right] \tag{6}$$

$$\rho \frac{\partial V_2}{\partial t} = - \frac{\partial P}{\partial x_2} + \left[\frac{\partial \tau_{12}}{\partial x_1} + \frac{\partial \tau_{22}}{\partial x_2} + \frac{\partial \tau_{32}}{\partial x_3} \right] \tag{7}$$

$$\rho \frac{\partial V_3}{\partial t} = - \frac{\partial P}{\partial x_1} + \left[\frac{\partial \tau_{13}}{\partial x_1} + \frac{\partial \tau_{23}}{\partial x_2} + \frac{\partial \tau_{33}}{\partial x_3} \right] \tag{8}$$

Cooling analysis. The analysis of the cooling process considers the relationship of the plastic flow distribution and heat transmission. The homogenous mould temperature and the sequence of filling will be affected by the shrinkage of the product formed. If the temperature is distributed non-uniformly, it tends to produce warp. This is mainly due to heat-transfer and crystallisation heat of the plastic.

$$\rho C_P \frac{\partial T}{\partial t} = k\left[\frac{\partial^2 T}{\partial x_1^2} + \frac{\partial^2 T}{\partial x_2^2} + \frac{\partial^2 T}{\partial x_3^3}\right] + \rho C_P r \Delta H \tag{9}$$

r = crystallisation rate; ΔH = crystallisation heat

3. Abductive Network Synthesis and Evaluation

Miller [22] observed that human behaviour limits the amount of information considered at a time. The input data are summarised and then the summarised information is passed to a higher reasoning level.

In an abductive network, a complex system can be decomposed into smaller, simpler subsystems grouped into several layers using polynomial function nodes. These nodes evaluate the limited number of inputs by a polynomial function and generate an output to serve as an input to subsequent nodes of the next layer. These polynomial functional nodes are specified as follows:

1. Normaliser

A normaliser transforms the original input variables into a relatively common region.

$$a_1 = q_0 + q_1 x_1 \tag{10}$$

Where a_1 is the normalised input, q_0, q_1 are the coefficients of the normaliser, and x_1 is the original input.

2. White node

A white node consists of linear weighted sums of all the outputs of the previous layer.

$$b_1 = r_0 + r_1 y_1 + r_2 y_2 + r_3 y_3 + \ldots + r_n y_n \tag{11}$$

Where y_1, y_2, y_3, y_n are the input of the previous layer, b_1 is the output of the node, and the r_0, r_1, r_2, r_3, …, r_n are the coefficients of the triple node.

3. Single, double, and triple nodes

These names are based on the number of input variables. The algebraic form of each of these nodes is shown in the following:

$$\text{single: } c_1 = s_0 + s_1 z_1 + s_2 z_1^2 + s_3 z_1^3 \tag{12}$$

$$\text{double: } d_1 = t_0 + (t_1 n_1 + t_2 n_1^2 + t_3 n_1^3) + (t_4 n_2 + t_5 n_2^2 + t_6 n_2^3) + (t_7 n_1 n_2) \tag{13}$$

$$\text{triple: } e_1 = u_0 + (u_1 o_1 + u_2 o_1^2 + u_3 o_1^3) + (u_4 o_2 + u_5 o_2^2 + u_6 o_2^3) + (u_7 o_3 + u_8 o_3^2 + u_9 o_3^3) + u_{10} o_1 o_2 + u_{11} o_2 o_3 + u_{12} o_1 o_3 + u_{13} o_1 o_2 o_3 \tag{14}$$

where z_1, z_2, z_3, …, z_n, n_1, n_2, n_3, …, n_n, o_1, o_2, o_3, …, o_n are the input of the previous layer, c_1, d_1, and e_1 are the output of the node, and the s_0, s_1, s_2, s_3, …, s_n, t_0, s_1, t_2, t_3, …, t_n, u_0, u_1, u_2, u_3, …, u_n are the coefficients of the single, double, and triple nodes.

These nodes are third-degree polynomial Eq. and doubles and triples have cross-terms, allowing interaction among the node input variables.

4. Unitiser

On the other hand, a unitiser converts the output to a real output.

$$f_1 = v_0 + v_1 i_1 \tag{15}$$

Where i_1 is the output of the network, f_1 is the real output, and v_0 and v_1 are the coefficients of the unitiser.

4. Part-Surface Model

This study uses an actual industrial product as a sample, Fig. 1. The mould part surface is located at the maximum projection area. As shown in Fig. 1, the bottom is the widest plane and is chosen as the mould part surface. However, most important is the searching of gate position on the part surface.

This study establishes the parameter equation by using an abductive neuron network, in order to establish the simulated annealing method (SA) to find the optimal gate path position.

The parameter equation of a part-surface is expressed by $F(Y) = X$. First, use a CMM system to measure the XYZ coordinate values (in this study $z = 0$) of 22 points on the mould part-line on the mould part-surface as illustrated in Table 1, and the gate position is completely on the curve in this space.

Prior to developing a space-curve model, a database has to be trained, and a good relationship msut exist between the control point and abductive network system. A correct and

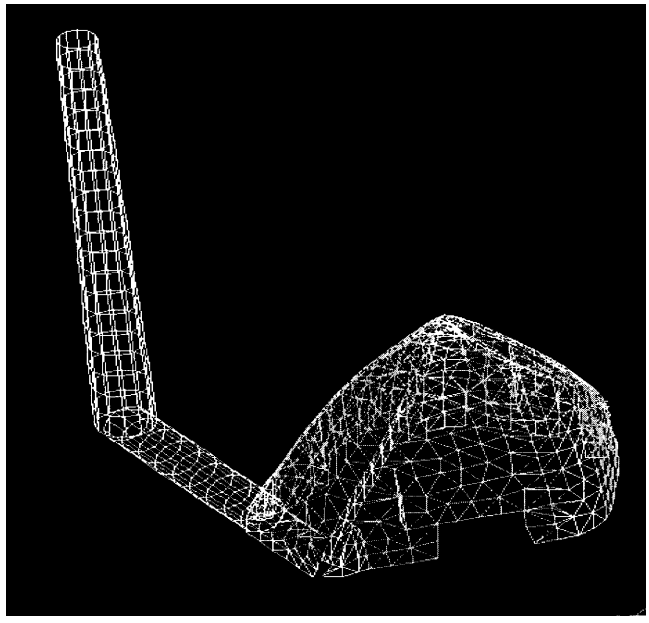

Fig. 1. Injection-mould product.

Table 1. *X, Y* coordinate.

Set number	*X*-coordinate	*Y*-coordinate
1	0.02	–4.6
2	–1.63	–4.33
3	–3.28	–3.5
4	–5.29	–2.04
5	–7.31	–0.56
6	–9.34	0.9
7	–11.33	2.35
8	–12.98	3.94
9	–13.85	5.57
10	–14.12	7.34
11	–13.69	9.67
12	–12.96	11.9
13	–10.00	21.03
14	–9.33	23.16
15	–8.64	25.28
16	–7.98	27.39
17	–7.87	28.31
18	–7.80	29.29
19	–7.83	30.34
20	–7.60	31.30
21	–7.07	32.15
22	–6.11	32.49

precise curve Eq. is helpful for finding the optimal gate location.

To build a complete abductive network, the first requirement is to train the database. The information given by the input and output parameters must be sufficient. A predicted square error (PSE) criterion is then used to determine automatically an optimal structure [23]. The PSE criterion is used to select the least complex but still accurate network.

The PSE is composed of two terms:

$$\mathrm{PSE} = \mathrm{FSE} + K_P \tag{16}$$

Where FSE is the average square error of the network for fitting the training data and K_P is the complex penalty of the network, shown by the following equation:

$$K_P = \mathrm{CPM}\,\frac{2\sigma_p^2 K}{N} \tag{17}$$

Where CPM is the complex penalty multiplier, K_P is a coefficient of the network; N is the number of training data to be used and σ_p^2 is a prior estimate of the model error variance.

Based on the development of the database and the prediction of the accuracy of the part-surface, a three-layer abductive network, which comprised design factors (input: various *Y* coordinate) and output factors (*X* coordinate) is synthesised automatically. It is capable of predicting accurately the space curve at any point under various control parameters. All polynomial equations used in this network are listed in Appendix A. (PSE = 5.8×10^{-3}).

Table 2 compares the error predicted by the abductive model and CMM measurement data. The measurement daa is excluded from the 22 sets of CMM measurement data for establishing the model. This set of data is used to test the appropriateness of the model established above. We can see from Table 2 that the error is approximately 2.13%, which shows that the model is suitable for this space curve.

Table 2. CMMS-coordinate and neural network predict compared (it is not included in any original 22 sets database).

Items	CMMS coordinate	neural network predict coordinate	Error values (CMMS-predict)/ CMMS
Coordinate	(–11.25, 16.0)	(–11.01, 16.0)	2.13%

5. Create the Injection-Mould Model

Similarly, the relationship is established between input parameters (gate location and gate size) and the output parameter (deformation) during the injection process. To build a complete abductive network, the first requirement is to train the database. The information given by the input and the output data must be sufficient. Thus, the training factor (gate location) for abductive network training should be satisfactory for making defect-free products. Figure 2 shows the simulation of FEM mould-flow. Table 3 shows the position of the gate and the maximum deformation of the product obtained from mould-flow analysis.

Based on the development of the injection-mould model, three-layer abductive networks, which are comprised of injection-mould conditions and the injection-results (deformation), are synthesised automatically. They are capable of predicting accurately the product strain (the result of injection-moulded product) under various control parameters. All polynomial equations used in this network are listed in Appendix B (PSE = 2.3×10^{-5}).

Table 4 compares the error predicted by the abductive model and the simulation case. The simulation case is excluded from the 22 sets of simulation cases for establishing the model. This set of data is used to test the appropriateness of the model established above. We can see from Table 4 that the error is

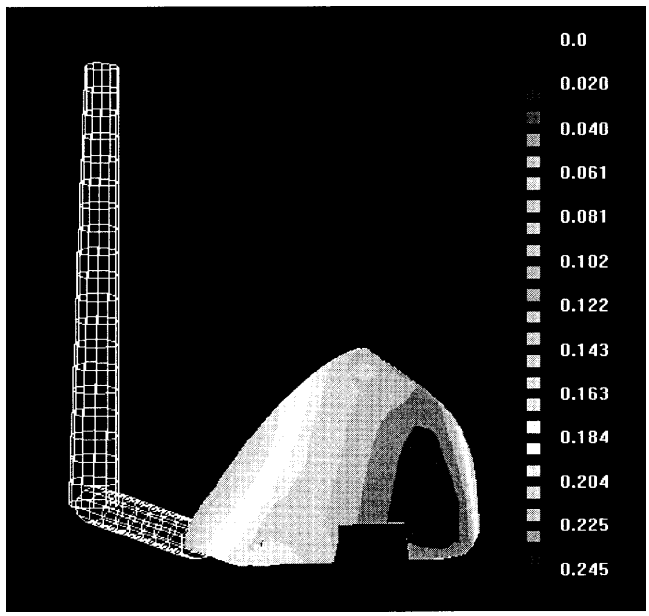

Fig. 2. The deformation of FEM mould-flow.

Table 3. Gate location and the maximum strain relationship.

Set number	*X*-coordinate	*Y*-coordinate	Gate width	Gate length	Produce max. strain
1	0.02	–4.6	0.525	1.1475	0.348
2	–1.63	–4.33	0.7	1.53	0.3153
3	–3.28	–3.5	0.875	1.9125	0.2710
4	–5.29	–2.04	1.05	2.295	0.2858
5	–7.31	–0.56	0.525	1.1475	0.3017
6	–9.34	0.9	0.7	1.53	0.526
7	–11.33	2.35	0.875	1.9125	0.2369
8	–12.98	3.94	1.05	2.295	0.2517
9	–13.85	5.57	0.525	1.1475	0.2788
10	–14.12	7.34	0.7	1.53	0.2773
11	–13.69	9.67	0.875	1.9125	0.2988
12	–12.96	11.9	1.05	2.295	0.2997
13	–10.00	21.03	0.525	1.1475	0.2576
14	–9.33	23.16	0.7	1.53	0.2624
15	–8.64	25.28	0.875	1.9125	0.2542
16	–7.98	27.39	1.05	2.295	0.2495
17	–7.87	28.31	0.525	1.1475	0.2503
18	–7.80	29.29	0.7	1.53	0.2456
19	–7.83	30.34	0.875	1.9125	0.2596
20	–7.60	31.30	1.05	2.295	0.2457
21	–7.07	32.15	0.525	1.1475	0.2499
22	–6.11	32.49	0.7	1.53	0.2511

Table 4. Mould-flow simulated and neural network predict compared (it is not included in any original 22 set database).

Items	FEM mould-flow simulation	Neural network predict
X-coordinate	–11.01	–11.01
Y-coordinate	16.0	16.0
Gate width	1.8	1.8
Gate height	0.9	0.9
Produce max. deformation	0.3178	0.3325
Error values (FEM-predict)/FEM		4.62%

approximately 4.62%, which shows that the model is suitable for this model requirement.

6. Simulation Annealing Theory

In 1983, a theory that was capable of solving the global optimisation problem was developed for the optimised problem. The concept was a powerful optimisation algorithm based on the annealing of a solid which solved the combinatorial optimisation problem of multiple variables. When the temperature is T and energy E, the thermal equilibrium of the system is a Boltzman distribution:

$$P_r = \frac{1}{Z(T)} \exp\left(\frac{-E}{K_B T}\right) \tag{18}$$

$Z(T)$ = normalisation factor; K_B = Boltzman constant; $\text{Exp}(-E/K_B T)$ = Boltzman factor

Metropolis [24] proposed a criterion for simulating the cooling of a solid to a new state of energy balance. The basic criterion used by Metropolis is an optimisation algorithm called "simulated annealing". The algorithm was developed by Kirkpatrick et al. [20].

In this paper, the simulation-annealing algorithm is used to search for the optimal control parameters for gate location. Figure 3 shows the flowchart of the simulated annealing search. First, the algorithm is given an initial temperature T_s and a final temperature T_e, and a set of initial process vectors O_x. The objective function *obj* is defined, based on the injection parameter performance index. The objective function can be recalculated for all the different perturbed compensation parameters. If the new objective function becomes smaller, the peturbed process parameters are accepted as the new process parameters and the temperature drops a little in scale. That is:

$$T_{i+1} = T_i C_T \tag{19}$$

where i is the index for the temperature decrement and the C_T is the decay ratio for the temperature ($C_T < 1$).

However, if the objective function becomes larger, the probability of acceptance of the perturbed process parameters is given as:

$$P_r(obj) = \exp\left[\frac{\Delta obj}{K_B T}\right] \tag{20}$$

Where K_B is the Boltzman constant and Δobj is the different in the objective function. The procedure is repeated until the temperature T_i approaches zero. It shows the energy dropping to the lowest state.

Once the model of the relationship among the functions of the gate location, the input parameters and output parameters are established, this model can be used to find the optimal parameter for the gate location. The optimal parameter for the process can be obtained by using the objective function to serve

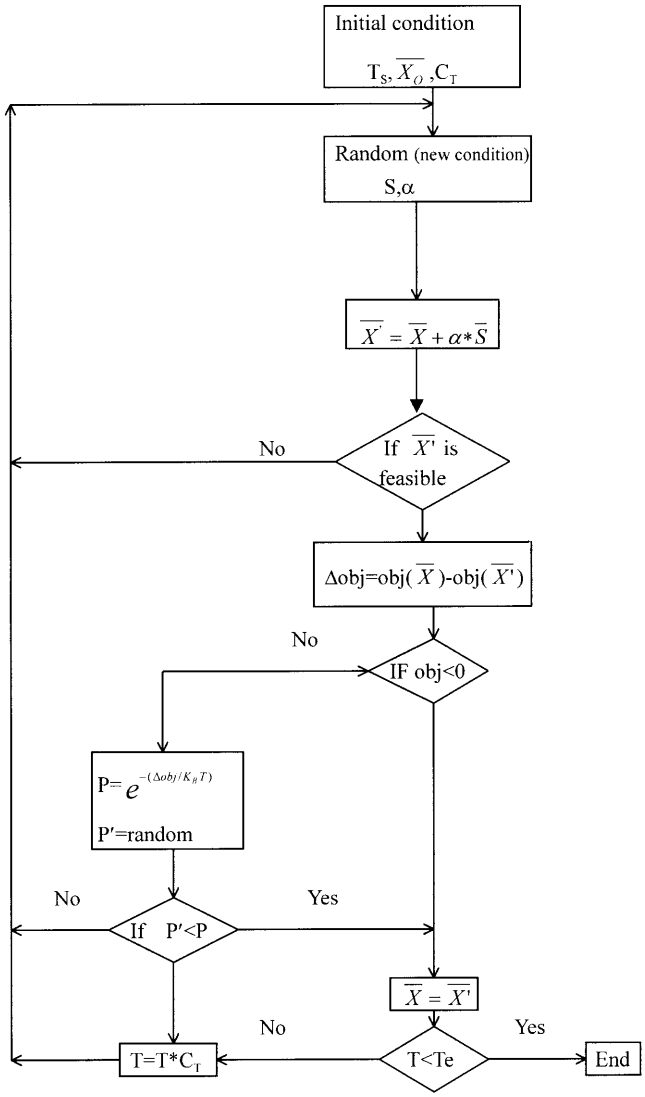

Fig. 3. Flowchart of the simulated annealing searching.

as a starting point. The objective function *obj* is formulated as follows:

$$obj = w_1 \times (X\text{-Coordinate}) + w_2 \times (Y\text{-Coordinate}) + w_3 \times (\text{Gate-wide size}) + w_3 \times (\text{Gate-height size}) \quad (21)$$

Where w_1, w_2, and w_3 are the weight functions.

The control parametric of the *X*, *Y* location should comply with the part-surface parameter equation. That means the basic condition of optimisation should fall within a certain range:

1. The *X*-coordinate value obtained from optimisation should be larger than the minimum *X*-coordinate value, and smaller than the maximum *X*-coordinate value.
2. The *Y*-coordinate value obtained from optimisation should be larger than the minimum *Y*-coordinate value, and smaller than the maximum *X*-coordinate value. The *X*, *Y*-coordinate depends on the Appendix A neural network equation.
3. The gate-wide size obtained from optimisation should be larger than the minimum size of gate-width, and smaller than the maximum gate-width size.
4. The gate-height size obtained from optimisation should be larger than the minimum size of gate-height, and smaller than the maximum gate-height size.

The inequalities are given as follows:

$$\text{The smallest } X \text{ coordinate value} < X \text{ coordinate value} < \text{the largest } X \text{ coordinate value} \quad (22)$$

$$\text{The smallest } Y \text{ coordinate value} < Y \text{ coordinate value} < \text{the largest } Y \text{ coordinate value} \quad (23)$$

$$\text{The smallest gate-width size} < \text{gate-width size} < \text{the largest-width gate size} \quad (24)$$

$$\text{The smallest gate-height size} < \text{gate-height size} < \text{the largest-height gate size} \quad (25)$$

The upper-bound conditions should be kept to an acceptable level so as to find the optimal (acccurate) gate coordinate.

7. Results and Discussion

An example of the simulation is used to illustrate the process of optimising the gate location. In the first case, the weight funtion $w_1 = w_2 = w_3 = w_4 = 1$ (the gate location and size is equal weight). In this case, the parameters used in the simulation annealing algorithm are given as: initial temperature T_s = 100°C, final temperature T_e = 0.0001°C, decay ratio C_T = 0.98, Boltzman constant K_s = 0.00667, and the upper bound of the *X*-coordinate is –0.0276 mm, upper bound of *Y*-coordinate is 32.49 mm (*X* depends on the *Y*-coordinate).

Simulated annealing is used for finding the optimal gate coordinates and gate size, as shown in Table 5. When gate size is w = 1.8 mm and h = 0.9 mm, the optimal gate location is Y = 30.0 mm, and X = –7.824 mm. Predicting the minimum deformation using the optimal parameters is about 0.2563 mm (minimum, Table 5).

In Fig. 4, for a fixed gate size w = 1.8 mm and the h = 0.9 mm, the optimal value is found by using the *Y*-coordinate variation. In Fig. 4, the *Y*-coordinate has the minimum deformation when the optimal parameter of the *Y*-coordinate is 30.0 mm (X = –7.824 mm), and the deformation is 0.2563 mm (minimum).

Table 5 shows a comparison between the simulation mould-flow error and the optimal value predicted by the model. The error is approximately 5.4%. In the foregoing discussion, it

Table 5. SA optimal parameters and FEM prediction compared (it is not included in any original 22 set database).

Items	FEM mould-flow simulation	SA optimal predict
X-coordinate	–7.824	–7.824
Y-coordinate	30.0	30.0
Gate width	1.8	1.8
Gate width	0.9	0.9
Produce max. deformation	0.271	0.2563
Error values (FEM-SA)/FEM		5.4%

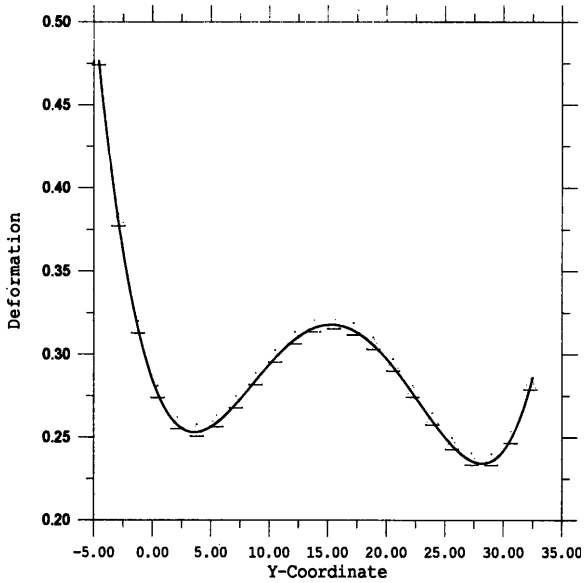

Fig. 4. Deformation and *Y*-coordinate relationship.

has been shown clearly that the process parameters for optimum bend performance can be systematically obtained through this approach.

8. Conclusion

This paper describes a neural network approach for modelling and optimisation of injection-mould gate parameters.

1. Comparing the value of errors using the finite-element method and abductive-network prediction we have designed the injection-mould model. Based on the best modelling using an abductive network, the complicated relationships between the injection-gate coordinate parameters and deformation performance can be obtained.
2. A global optimisation algorithm, called simulated annealing (SA), is then applied to the abductive network to obtain the optimal process parameters based on an objective function.
3. Lastly, a comparison is made between the FEM simulation mould-flow error values and model predicted values by the optimisation process. It shows that the model fits the FEM simulation mould-flow data and the finite-element and abductive-network predictions. Therefore, the rapidity and efficiency of determining optimal designing prameters for injection-moulding can be used successfully to improve the accuracy of the injection-mould design process.

References

1. S. M. Richardson, "Hele-Shaw flow with a free surface produced by the injection of fluid into a narrow channel", *J. Fluid Mech.* 56, pp. 609–618, 1972.
2. M. J. Crochet, A. R. Davies and K. Walters, Numerical Simulation of Non-Newtonian Flow, Elsevier, 1984.
3. R. B. Bird, R. C. Armstrong and O. Hassager, Dynamics of Polymeric Liquid, 1, Fluid Mechanics, 2nd edn, Elsevier, 1987.
4. R. B. Bird, R. C. Armstrong and O. Hassager, Dynamics of Polymeric Liquid, 2, Fluid Mechanics, 2nd edn, Elsevier, 1987.
5. Lapidus and G. F. Pinder, Numerical Simulation of Partial Differential Equation in Science and Engineering, McGraw-Hill, 1982.
6. L. T. Mazione, Applications of Computer Aided Engineering in Injection Molding, Hanser, 1987.
7. W. C. Bushko and V. K. Stokes, "Solidification of thermo-viscoelastic melts. Part II: Effect of processing conditions on shrinkage and residual stress", Polymer Engineering and Science, 36, pp. 352–364, 1996.
8. W. C. Bushko and V. K. Stokes, "Solidification of thermoviscoelastic melts: Part III: Effect of molds temperature difference on warpage and residual stress", Polymer Engineering and Science, 36, pp. 365–377, 1996.
9. W. C. Bushko and V. K. Stokes, "Solidification of thermoviscoelastic melts: Part IV: Effect of boundary conditions on shrinkage and residual stress", Polymer Engineering and Science, 32, pp. 658–671, 1996.
10. J. Greener, "Greener sequence of the packing place in injection molding", Polymer Engineering and Science, 26, pp. 886–895, 1986.
11. T. H. Kwon, "Mold cooling system design using boundary element method", ASME Journal of Engineering for Industry, 110, pp. 384–394, 1988.
12. K. Hinldsekhar, J. Lottey and K. K. Wang, "CAD of mold cooling in injection mold using a three-dimensional numerical simulation", Journal of Manufacturing Science and Engineering, 144, pp. 213–221, 1992.
13. S. J. Park, "Thermal and design sensitivity analyses for cooling system of injection mold. Part I: Thermal analysis", Journal of Manufacturing Science and Engineering, 120, pp. 287–295, 1998.
14. S. J. Park, "Thermal and design sensitivity analyses for cooling system of injection mold. Part II: Design sensitivity analysis", Journal of Manufacturing Science and Engineering, 120, pp. 296–306, 1998.
15. Marc Weinstein and Souran Manoochehri, Optimum Parting Line Design of Molded and Cast Parts for Manufacturability, Journal of Manufacturing Systems, 16, pp. 1–12, 1997.
16. L. L. Chen and S. Y. Chou, "Optimal parting directions by partial visibility", Proceedings of ASMS Winter Annual Meeting, 59, pp. 17–25, 1992.
17. L. L. Chen and S. Y. Chou, "Parting directions for mould and die design", Journal of Computer-Aided Design, 25, pp. 762–768, 1993.
18. J. C. Lin and C. C. Tai, "The position of optimal injection gate choose of the die-casting die, Journal of Materials Processing Manufacturing Technology, 86, pp. 87–100, 1999.
19. G. J. Montgomery and K. C. Drake, "Abductive reasoning network", Neurocomputing, 2, pp. 97–104, 1991.
20. S. Kirkpatrick, C. D. Gelatt and M. P. Vecchi, "Optimization by simulated annealing", Science, 220(4958), pp. 671–680, 1983.
21. S. Geman and D. Geman, "Stochastic relaxation, Gibbs distributions and the Bayesian restoration of images", IEEE Transactions on Pattern Analysis and Machine Intelligence, 6(6), pp. 721–741, 1984.
22. W. Lee and B. J. Sheu, Hardware Annealing in Analog VLSI Neurocomputing, Kluwer, 1991.
23. C. Zhang and H. P. Wang, The Discrete Tolerance Optimal Problem, ASME Manufacturing Review, 6(1), pp. 60–71, 1991.
24. Y. S. Trang, S. C. Ma and L. K. Chung, "Determination of optimal cutting parameters in wire electrical discharge machining", International Journal of Machine Tools and Manufacture, 35(12), pp. 1693–1701, 1995.
25. C. C. Tai and J. C. Lin, "The optimization deep-draw clearance design to the deep-draw die", International Journal of Advanced Manufacturing Technology, 14, pp. 390–398, 1998.
26. C. C. Tai and J. C. Lin, "A runner-optimization study of a die-casting die", Journal of Materials Processing Technology, 84, pp. 1–12, 1998.

Appendix A

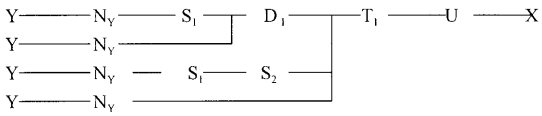

(N : Normalizer Node, S: Single Node, D: Double Node, T: Triple Node U: Untizer Node)(PSE=$5.8X10^{-5}$)

$N_Y = -0.997433 + 0.0713889*Y$

$S_1 = 0 - 1.298 + 1.104* N_Y + 1.40* N_Y^2 - 1.0* N_Y^3$;

$D_1 = -0.60 + 0.12*S_1 + 0.092*N_Y - 0.154*S_1*S_1 + 0.696* N_Y * N_Y - 0.67*S_1* N_Y + 0.016*S_1^3$;

$S_2 = -0.012 + 1.01*S_1 + 0.0146376* S_1^2 - 0.06* S_1^3$;

$T_1 = 0 + 49758.7 + 11610.9*D1 + 30882.8*S_2 - 37056.4* N_Y + 218.493*D_1^2 + 1059.22*S_2^2 - 53985* N_Y^2 + 116.344*D_1*S_2 - 197.683*D_1* N_Y + 7850.49*S_2* N_Y + 14.7273*N_Y *S_2*D_1 + 2.42825*D_1^3 - 25.4517*S_2^3 + 32667.5*N_Y^3$;

$U = -8.454 + 3.83*T_1$;

$X = U$

Appendix B

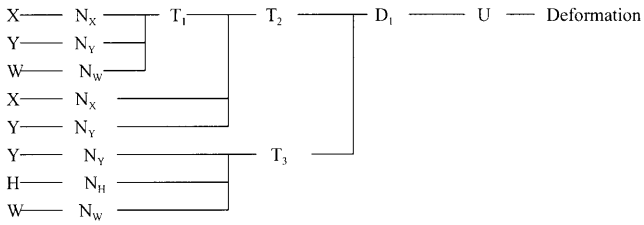

(PSE=$2.3X10^{-5}$)

$N_X = 2.20872 + 0.26126*X$; $N_Y = -0.997433 + 0.0713889*Y$;

$N_W = -3.86574 + 2.2922*W$; $N_H = -3.86574 + 5.01009*H$;

$T_1 = 1.49 - 1.31N_X - 2.98*N_Y - 1.24*N_W - 0.798*N_X^2 - 0.90*N_Y - 0.37*N_W^2 - 1.12*N_X^2 - 0.34*N_X*N_W + 0.38*N_Y*N_W - 0.95*N_X*N_Y*N_W + 0.7*N_X^3 + 2.17314*N_Y^3 + 0.713014*N_W^3$;

$T_2 = 0.51 - 0.027*T_1 + 0.75*N_X - 1.01*N_Y + 0.27*T_1*T_1 + 0.167*N_X^2 - 1.16*N_Y^2 + 0.015*T_1*N_X - 0.09*T_1*N_Y - 0.58*N_X*N_Y - 0.185*T_1*N_X*N_Y + 0.28*T_1^3 - 0.165*N_X^3 + 0.98*N_Y^3$;

$T_3 = 0 + 0.226 - 0.87*N_Y - 1.08*N_H - 0.016*N_Y^2 - 0.31*N_H^2 + 0.2*N_Y*N_H + 0.158*N_Y*N_W*N_H + 0.187*N_Y^3 + 0.47*N_H^3 + 0.114*N_W^3$;

$D_1 = 0.04 + 1.02*T_2 + 0.19*T_3 - 0.123*T_2*T_2 - 0.07*T_3^2 + 0.23*T_2*T_3 + 0.02*T_2^3 - 0.254967*T_3^3$;

$U = 0.28 + 0.061*D_1$;

Deformation =U